Journal of Mechanical Engineering Research and Developments
ISSN: 1024-1752
CODEN: JERDFO
Vol. 43, No.7, pp. 75-86
Published Year 2020

Numerical Simulation of Flow Around the Ship Using CFD Method

Ngoc Kien Vu, Hong Quang Nguyen*

Thai Nguyen University of Technology, 666, 3/2 Street, Tich Luong Ward, Thai Nguyen City, Vietnam

Corresponding Author Emaill: quang.nguyenhong@tnut.edu.vn

ABSTRACT: The paper describes the results of calculation of ship resistance, dynamic sinkage and trim in calm water condition by solving unsteady Reynolds Averaged Navier-Stockes equation (RANSE). The free surface is modeled by applying Volume-of-Fluid method. To achieve a high level of accuracy at some certain cells, the unstructured hexahedral grid type has been employed and locally refined in the importance regions. The effect of grid size, y+ value on the predicted results are analyzed. It is indicated that the satisfied accuracy can be obtained with meshes of lower million cells generated for half of the ship geometry. The well-known KCS containership is applied to verify and validate the accuracy of case studies.

KEYWORDS: RANSE, Resistance, CFD, trim, sinkage.

INTRODUCTION

In ship hydrodynamics computation, the problem of determining the ship resistance is a key factor in the design of the propulsion system. As it involves estimating the ship required horsepower to gain the design speed. In order to achieve a reliable result for ship resistance prediction, it is necessary to perform the model tests in towing tank. The obtained measured results then it will be extrapolated to the full scale based on extrapolation methods has been proposed by International Towing Tank Conference (ITTC) [1]. Nevertheless, the experimental method has disadvantage are time and cost consuming due to both model manufacturing and the experiment itself. Hence, this method is not used in the initial ship design stage.

Nowadays, Computational Fluid Dynamics (CFD) has made a considerable progress in the field prediction of ship hydrodynamics in general and ship resistance in particular. With the fast advance of computational resources, CFD methods have been widely used in ship designing and ship resistance predictions. CFD methods provides relatively accurate results, fast and inexpensive in comparison with the experimental method. Moreover, they can provide the visualization of flow quantities, i.e. wall shear stress, pressure distribution on ship hull, wave elevation contour and streamlines, which provide designers information to develop or improve ship hull form with respect to minimize ship resistance. The group of CFD methods applied to predict ship hydrodynamics characteristics includes: Large Eddy Simulation, Potential flow theory and Reynolds Averaged Navier-Stokes equations (RANSE). At the moment, the most popular method is widely used in predict ship resistance is the RANSE method, since it gives a sufficient level of accuracy of obtained results for engineering purposes at acceptable computational time [2-10]. Hence, this paper uses the RANSE method for simulation flow around the ship.

Some useful results applying the RANSE method for simulation flow around the ship have been already achieved by researchers. A group researcher used RANSE method with different turbulence models to study their influence on ship resistance results flow around the ship [11]. Some researchers have carried out comparison of turbulence models for prediction of wake around the ship [12,13]. In other hand, researchers performed uncertainty analysis in ship resistance evaluation for different ship model [14]. In a study also they have used RANSE method with turbulence model SST k-ω to predict the ship resistance for DTMB vessel [15]. The deviation between the predicted results and the measured value varies from 1.25 to 3.86%. Chengsheng et al. [16] used RANSE method with k-ε turbulence model to evaluate the ship resistance for DTMB vessel ship in model scale ranges from 0.12 to 2.36%. The error between the calculated results and the measured data is less than 4% in all range of Froude

numbers. Tu TN et al. [17] applied RANSE method with standard k- ε turbulence model to predict the ship resistance for DTMB vessel in model scale.

The deviation between predicted and experimental results is less than 3.5%. Those previous researches mentioned above gives a helpful data source for the further research flow around ship using RANSE method. However, those above studies have not yet evaluated the effect y+ value on the predicted results, which has a considerable impact on numerical obtained results [18]. In addition, the effect of Froude numbers on wave pattern around the ship was unaddressed in those researches. Thus, the objectives of this paper are to focus on simulation flow around the ship by solving unsteady RANSE. The free surface is modeled by applying the Volume-of-Fluid method. The factors that effect on predicted numerical obtained results such as grid size and y+ value are analyzed. Moreover, the effect of Froude numbers on wave pattern around the ship and wall shear stress distribution on ship hull is indicated in this study. The well-known KCS containership is applied to verify and validate the accuracy of case studies.

MATERIALS AND METHODS

Governing equation

The governing equations for the turbulent flow are the instantaneous conservation of mass and momentum, which are defined as follows [19]:

$$\frac{\partial U_i}{\partial x_i} = 0 \tag{1}$$

$$\rho \frac{\partial u_i}{\partial t} + \rho U_j \frac{\partial U_i}{\partial x_j}\left(u_i u_j\right) = -\frac{\partial P}{\partial x_i} + \frac{\partial}{\partial x_j}\left(\mu \frac{\partial U_i}{\partial x_j} - \rho \overline{u_i' u_j'}\right) + f_i \tag{2}$$

where $U_i = (U,V,W)$ represents the velocity component in $x_i = (x,y,z)$ direction, while ρ, p, μ, f_i and $-\rho\overline{u_i' u_j'}$ are density of fluid, the static pressure, fluid viscosity, body forces per unit volume and Reynolds stresses tensor, and body forces per unit, respectively.

Turbulence model

In this paper Realizable K-ε turbulence models are used because this turbulence model indicates to be capable to evaluate ship resistance accurately [20, 21].
For Realizable K-ε turbulence models, two equation are solved, including *k* and *ε*, while eddy viscosity is defined by following equation [22]:

$$\mu_t = \rho C_\mu \frac{k^2}{\varepsilon} \tag{3}$$

Where C_μ is the critical coefficient of model.

The transport equations are determined as follows [22]:

$$\frac{d}{dt}\int_V \rho k dV + \int_A \rho k(u_i - u_{gi}) da_i = \int_A \left(\mu + \frac{\mu_t}{\sigma_k}\right)\frac{\partial k}{\partial x_i} da_i + \int_V [f_c G_k - G_b - \rho(\varepsilon - \varepsilon_0) + \gamma_M + S_k] dV \tag{4}$$

$$\frac{d}{dt}\int_V \rho \varepsilon dV + \int_A \rho \varepsilon(u_i - u_{gi}) da_i = \int_A \left(\mu + \frac{\mu_t}{\sigma_\varepsilon}\right)\frac{\partial \varepsilon}{\partial x_i} da_i + \int_V [f_c C_{\varepsilon 1} S\varepsilon + \frac{\varepsilon}{k}(C_{\varepsilon 1} C_{\varepsilon 3} G_b) - \frac{\varepsilon}{k + \sqrt{\nu\varepsilon}} C_{\varepsilon 2}\rho(\varepsilon - \varepsilon_0) + S_\varepsilon] dV \tag{5}$$

where V is the cell volume, u_i is the vector of velocity, f_c is the correction factor of curvature, u_{gi} is the mesh velocity vector, a_i is the face of area vector, G_k is the turbulent production term, σ_k and σ_ε are turbulent

numbers, G_{nl} is the non-linear production term, G_b is linear the production term, γ_M is the dilatation dissipation, S_k and S_ε are user specified source terms, ν is the kinematic viscosity, $C_{\varepsilon 1}$, $C_{\varepsilon 2}$ and $C_{\varepsilon 3}$ are model coefficients, ε_0 is the ambient turbulence value in the source terms that counteracts turbulence decay and S is the modulus of the mean strain rate tensor.

NUMERICAL SIMULATION

Reference vessel

The container ship KCS without appended in model scale is used as reference vessel in this paper. The geometry of KCS containership and ship particulars are displayed in Table 1 and Figure 1.

Figure 1. Geometry of KCS containership [23]

Table 1. Main particulars of the DTMB [23]

Description		**Ship**	**Model**
Scale factor	λ	-	30.45
Length between perpendiculars	L_{PP} (m)	230.00	7.553
Length of waterline	L_{WL} (m)	232.50	7.635
Breadth at waterline	B_{WL} (m)	32.20	1.057
Draft	T (m)	10.80	0.355
Volume	∇ (m^3)	52030	1.843
Block coefficient	CB	0.651	0.651
Area of wetted surface	SW (m^2)	9530	10.28
Relative longitudinal center of buoyancy from midship section, "+" to fore	LCB (%Lpp), fwd+	-1.48	

Numerical setup

For ship resistance simulation, as the ship is symmetrical in geometry hence only half of the ship hull is simulated. The size of computed domain was set following the recommendations of ITTC [24]. It extended from -19.0 m to 19.0 m in upstream, from -19.0 m to 9.0 m in top and bottom directions and from 0 to 19.0 m in side direction, respectively. The coordinate origin located at aft perpendicular of the ship and free surface (0.355 m above keel). Moreover, the side boundary is taken parallel to the ship hull symmetry plane and treated as symmetry one. At the out flow boundary, hydrostatic pressure corresponding to the undisturbed water surface was specified. In flow, top and bottom boundaries were considered as inlets with prescribed velocity and volume fraction.

The trimmed grids with local adjustments and prism layers along the near-walls were applied in this research. The mesh is generated by determining the base mesh size, involving all spacing (the size of cell in various locations, the thickness of prism layer, etc.) are determined. Finer grids with the same topology are automatically made by just decreasing the size of the base mesh. To reduce the total cell number, fine mesh is unapplied in unnecessary locations (like in front and behind of hull and at larger distance above and below on each side of the ship hull). The local volume meshes was generated with different shapes and cell sizes, resulting in grid structure displayed in Figure. 2 for the medium mesh. The coarse, medium and fine grid had 0.87, 1.65 and 3.24 million cells, respectively. There were 7 prism layers along walls and the thickness of next-to-wall cells was 0.95 mm (the prism layer total thickness was 22 mm, the ratio of cell expansion was 1.45).

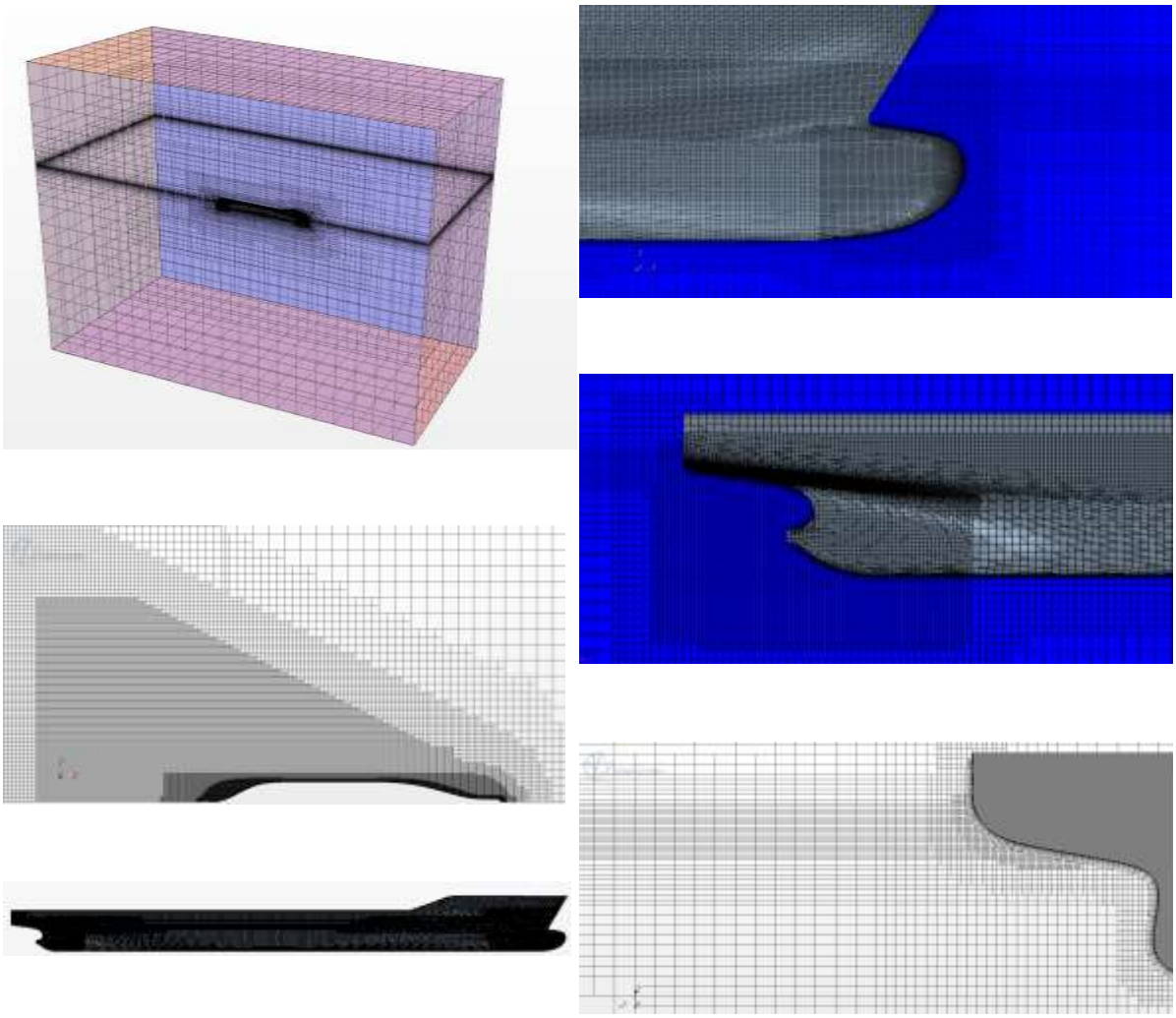

Figure 2. The structure of the medium grid around KCS container ship

For physics model, the simulation is performed using incompressible viscous unsteady RANSE. The 2-DOF motion are used to allow ship free to heave and pitch. VOF multiphase model is applied to handle the free surface wave flow around ship hull. Motion of the hull is captured during the simulation by applying DFBI Equilibrium option. Wave damping in the location distanced about 1.50 ship length away from the ship hull was used in order to reduce the force fluctuation due to wave reflections within the domain.

Choice of time step

One of the importance factor effect on numerical accuracy is choosing time step sizes. For implicit solvers, the time step size is decided by the flow features and also depend on the complexity of the turbulence model. For Realizable K-ε turbulence models, the time step is choice based on recommendation of ITTC [25] by Equation (6)

$$\Delta t = 0.005 \sim 0.01 L / U \tag{6}$$

Where U is the ship speed of ship, m/s and L is a ship length, m.

RESULTS AND DISCUSSIONS

The result of case study, in which the hull is free to heave and pitch, is presented in this section. The Froude number of the ship equals 0.26. The calculations were conducted in a time-marching mode, beginning with a calm water surface. The time step was set equal 0.04s and 10 iterations were carried out at each time level. The half

bare hull mass was set as 921.5 kg, the longitudinal center of gravity was set at x = 3.665m. Table 2 shows the numerical predicted total ship resistance at different mesh sizes. The experimental value of R_T equals 93.00 N [26] and the numbers in parentheses show percentage discrepancy between predicted and measured value ("+" indicates that the measured value is bigger than predicted one). The calculated total ship resistance is about 2.50% of the measured value and 7.74% for trim and sinkage on all mesh sizes. The discrepancy reduce from 2.366% to 0.903% with grid refinement. The change of measured values obtained from a coarse to a medium, and to a fine grid is monotonic. The maximum discrepancy regarding experimental value is obtained on coarse grid. The pressure resistance component increase monotonically together with mesh refinement, the frictional resistance component is smallest on the fine grid. Obviously, that change can be observed, typically when unstructured trimmed mesh, locally refined grids are applied.
Convergence ratio is defined as follows:

$$R_G = \frac{\varepsilon_{21}}{\varepsilon_{32}} \tag{7}$$

Where $\varepsilon_{21} = S_2 - S_1$ and $\varepsilon_{32} = S_3 - S_2$ are the discrepancy between predicted value achieved using medium grid (S_2) and fine grid (S_1) and the discrepancy between predicted achieved using coarse (S_3) grid and medium (S_2) grid. There are three kinds of possible convergence conditions: divergence ($R_G > 1$), oscillatory convergence ($R_G < 0$), and monotonic convergence ($0 < R_G < 1$). In this study, all three grids have the same quantity of prism layers: grid refinement was created by decreasing the cell size by a factor of 1.45 in all directions for outside prism layer cells, and only in the two tangential directions for the ones inside the prism layers. The average y+ values on the submerged ship hull equal to 50.

Table 2. Predicted total ship resistance on different mesh sizes

Parameter		EFD [26]	V&V study			ε_{21}	ε_{32}	R_G
			Grid #3	Grid #2	Grid #1			
R_T [N]	Value	93.00	95.20	94.34	93.84	0.50	0.86	0.58
	E%D	/	-2.366	-1.441	-0.903	/	/	/
C_F [N]	Value	/	73.21	72.42	71.98	0.44	0.79	0.56
	E%D	/	/	/	/	/	/	/
C_P [N]	Value	/	21.99	21.92	21.86	0.06	0.07	0.86
	E%D	/	/	/	/	/	/	/
Trim, [deg,]	Value	0.155	0.167	0.151	0.150	0.06	0.07	0.86
	E%D	/	-7.74	2.58	3.23	/	/	/
Sinkage, [mm]	Value	-15.50	-16.60	-15.20	-14.82	-0.38	-1.40	0.27
	E%D	/	-7.10	1.94	4.39	/	/	/

The impact of grid densities on numerical predicted results obtained from Table 2 can be explained by difference in wall shear stress distribution on ship hull and in the wave pattern around KCS ship for different grid densities (see Fig.3 and Fig.4.).

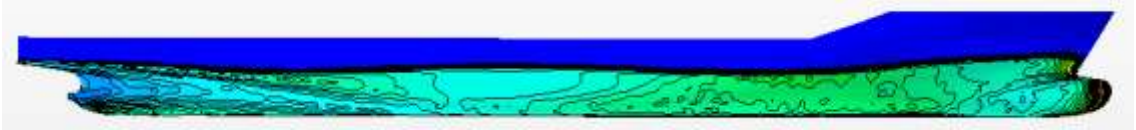

a) Coarse grid

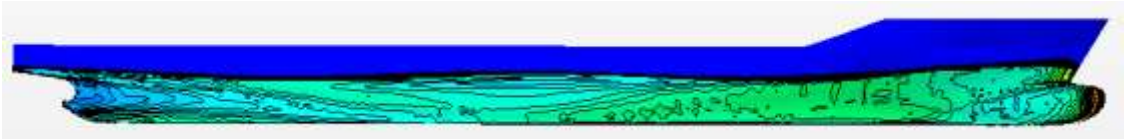

b) Medium grid

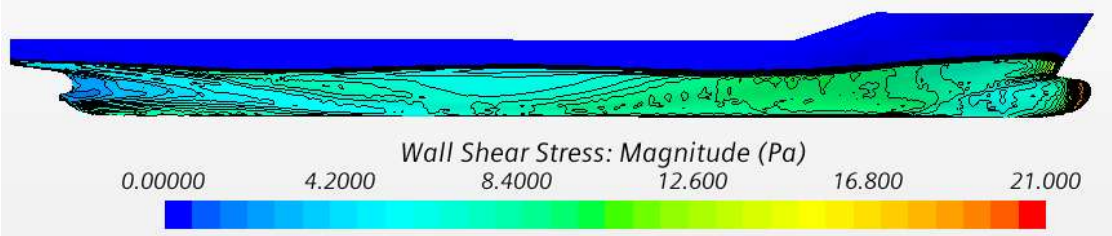

c) Fine grid

Figure 3. Predicted wall shear stress around the ship for different grid densities at Froude number 0.260

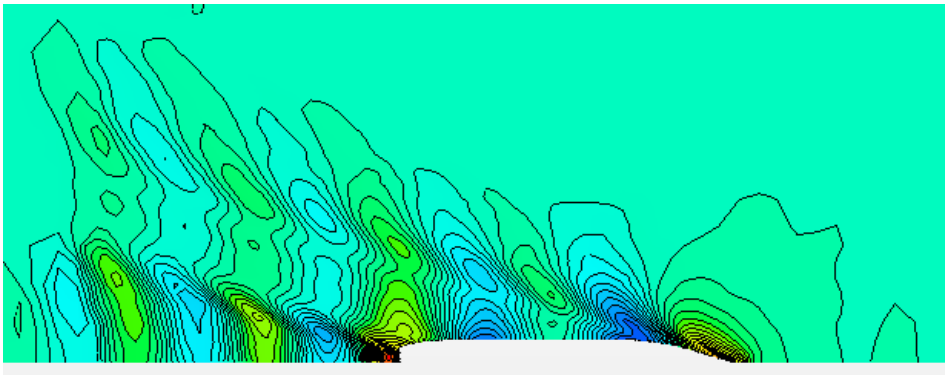

a) Coarse grid

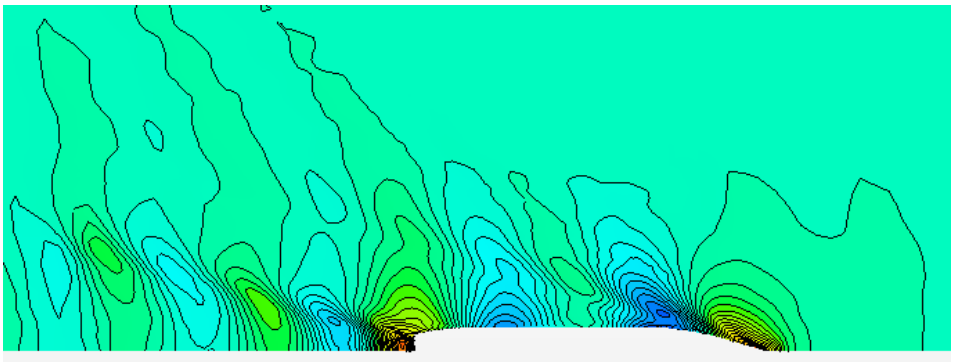

b) Medium grid

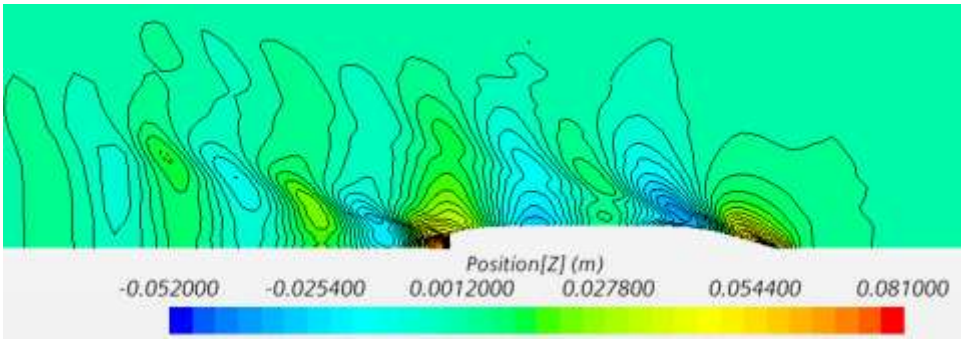

c) Fine grid

Figure 4. Predicted wave elevation around the ship for different grid densities at Froude number 0.260

Figures 5 and 6 display a history of convergence of heave and pitch motions of the ship and forces exerted on it for medium-mesh at Froude number of 0.260. Figure 5 shows how ship resistance components converge towards the unsteady-state solution. From Figure 5, we can observe the frictional resistance component rapidly stabilize

to a constant value, the pressure resistance component oscillates around the unsteady-state value with a diminishing amplitude.

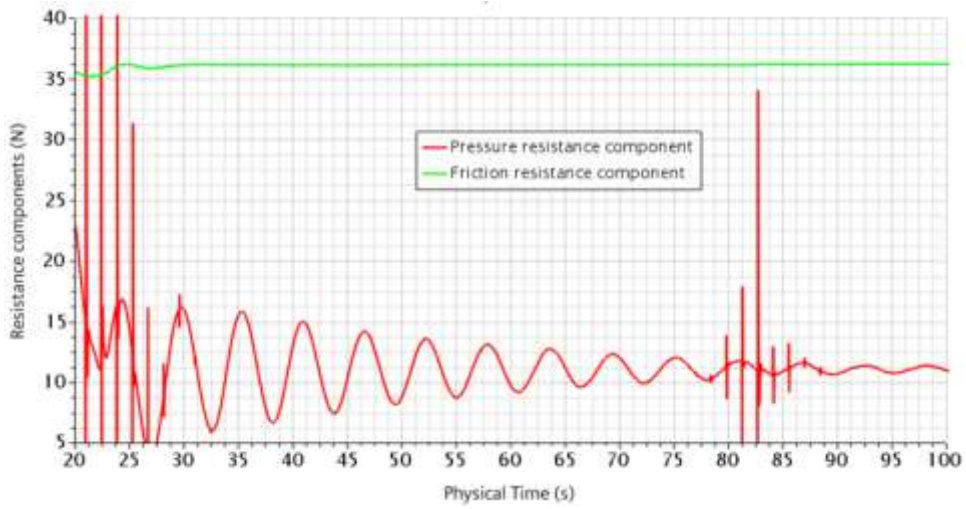

Figure 5. Convergence of friction and pressure resistance components during simulation process for medium mesh at Fr=0.260

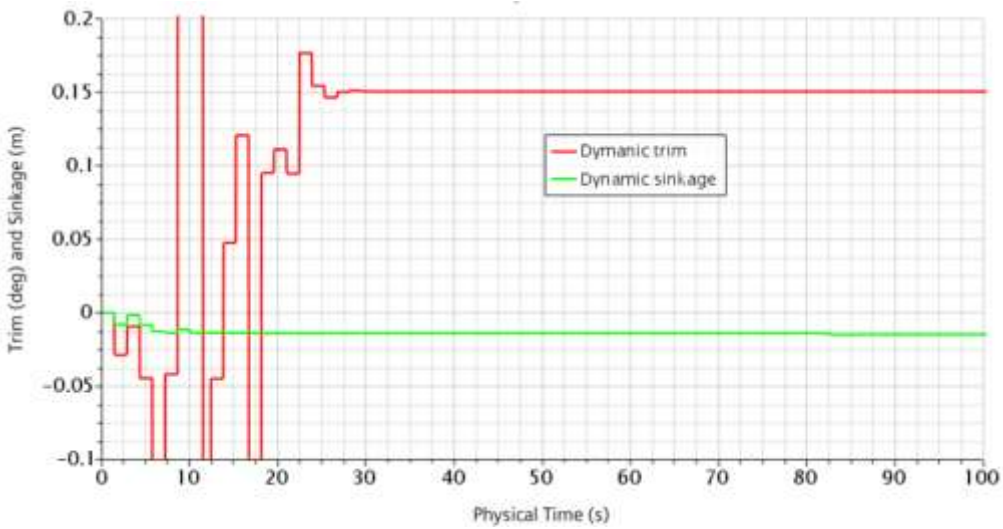

Figure 6. Convergence of pitch and heave motions for during simulation process for medium mesh at Fr=0.260

To investigate the effect of y+ on the numerical obtained results, the mesh is created with 5 prism layers instead of 7 prism layers. The expansion factor remained the same. However, the thickness of near-wall cell is 2.65 mm (compared to 1.2 mm in the case of generating 7 prism layers) in order to keep average $y+$ values between 100 and 120 over most of the submerged hull. The effect of y+ value on predicted ship resistance for two case study at Fr=0.260 are showed in Table 3.

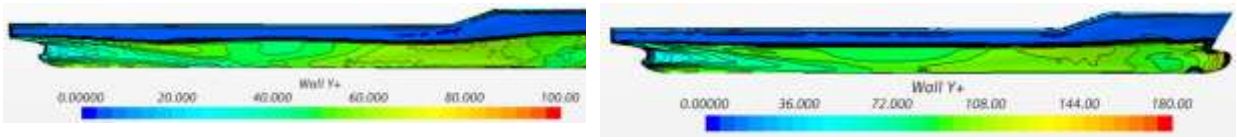

a) average $y+$ for case study 1 b) average $y+$ for case study 2

Figure 7. Y+ distribution on submerged ship hull

Table 3. Effect of y+ value on numerical predicted ship resistance

Parameter		**EFD [26]**	**CFD**	
			Average y + =50	*Average y + =120*
R_T [N]	Value	93.00	94.34	96.60
	E%D	/	-1.44	-3.87
R_F [N]	Value	/	72.42	74.29
	E%D	/	/	/
R_P [N]	Value	/	21.92	22.31
	E%D	/	/	/

As can be seen in Table 3, the predicted total ship resistance computed with setup average y+ value equal 50 provides more level of accuracy than *average* y+ value equal 120. The next step in this study, simulations were conducted for four Froude numbers, including: 0.195, 0.228, 0.260 and 0.280. For all case studies, computation was carried out on the medium mesh and average y+ value equal 50. The time step was selected follow Equation (6). Table 4 and Figure 8, 9 and 10 shows the comparison of calculated and experimental total ship resistance, dynamic trim and sinkage. As can be seen from Table 4, the predicted total ship resistance agrees well with measured data in towing tank. The biggest error is 3.60% for Froude number 0.195. The smallest error is 0.68% for Froude number 0.228. The dynamic sinkage and trim and differ more from measured value. The smallest error in trim and sinkage are 2.58% and 1.94% for Fr=0.260, respectively. The biggest error in trim and sinkage are 6.92% and 4.23% for Fr=0.280, respectively

Table 4. Predicted total ship resistance, trim and sinkage in comparison to experimental data

Froude numbers	**Total resistance [N]**			**Dynamic trim [deg.]**			**Dynamic Sinkage [mm]**		
	CFD	**EFD**	**E%D [%]**	**CFD**	**EFD**	**E%D [%]**	**CFD**	**EFD**	**E%D [%]**
0.195	51.28	49.50	-3.60	0.086	0.09	4.44	-8.52	-8.3	-2.65
0.228	65.24	64.80	-0.68	0.105	0.11	4.55	-10.68	-10.3	-3.69
0.260	94.34	93.00	-1.44	0.151	0.155	2.58	-15.2	-15.5	1.94
0.280	134.8	133.30	-1.13	0.139	0.13	-6.92	-18.58	-19.4	4.23

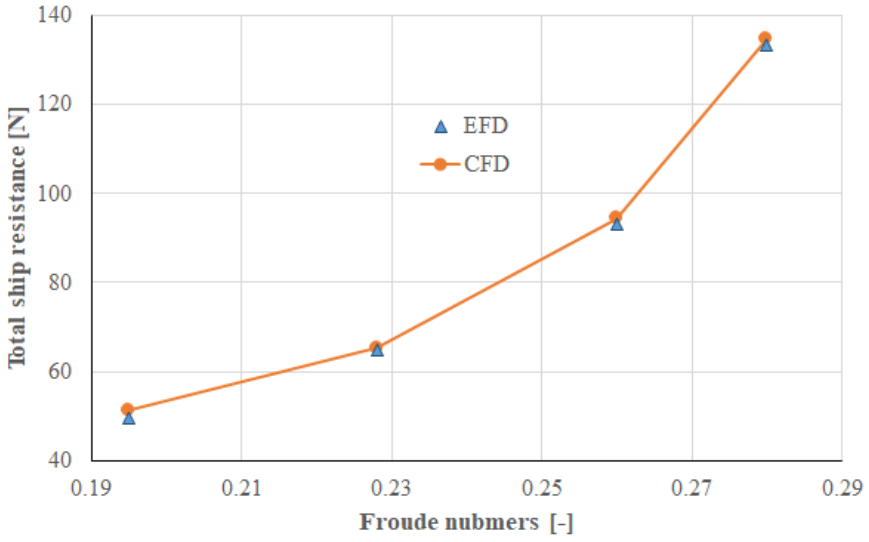

Figure 8. Comparison of calculated and measured total ship resistance

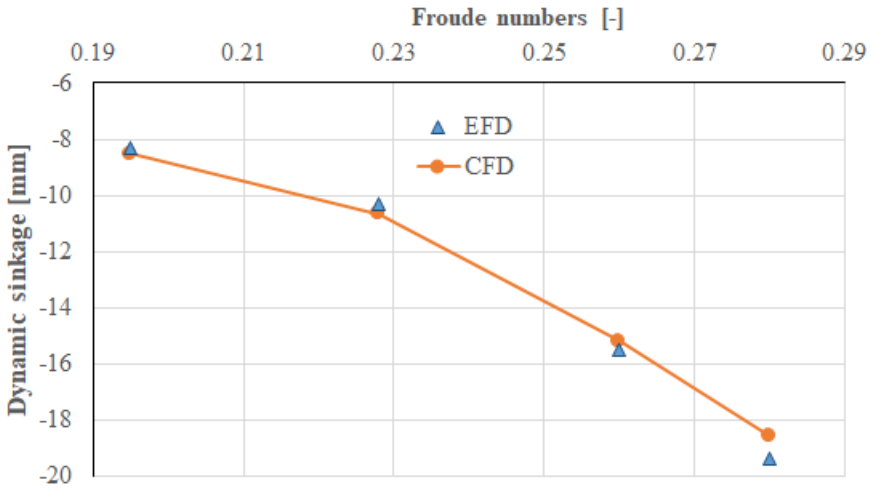

Figure 9. Comparison of calculated and measured dynamic sinkage

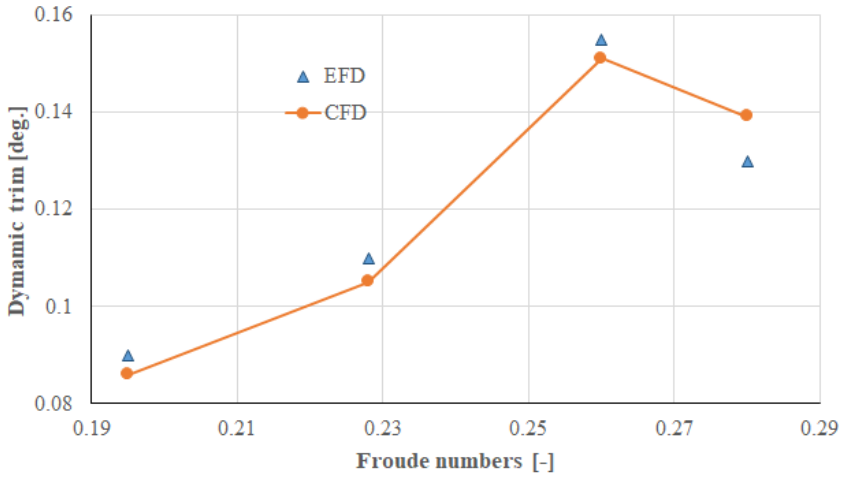

Figure 10. Comparison of calculated and measured dynamic trim

Figure 11 demonstrates the predicted wave elevation patterns around the ship at four values of Froude numbers. It can be observed from Figure 11 that, wave elevation patterns appear differently at different Froude numbers. The highest water elevation is always appeared in front of the ship, ranging from 0.0436 m at Fr = 0.1950 to 0.0917 m at Fr = 0.280. Meanwhile, the minimum one located at hull shoulder, ranging from -0.0178m at Fr=0.1950 to -0.056m at Fr=0.280.

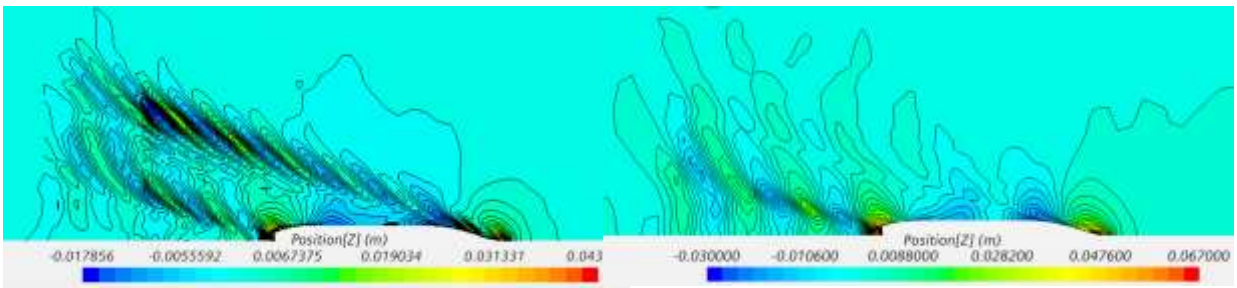

a) Fr=0.195 b) Fr=0.228

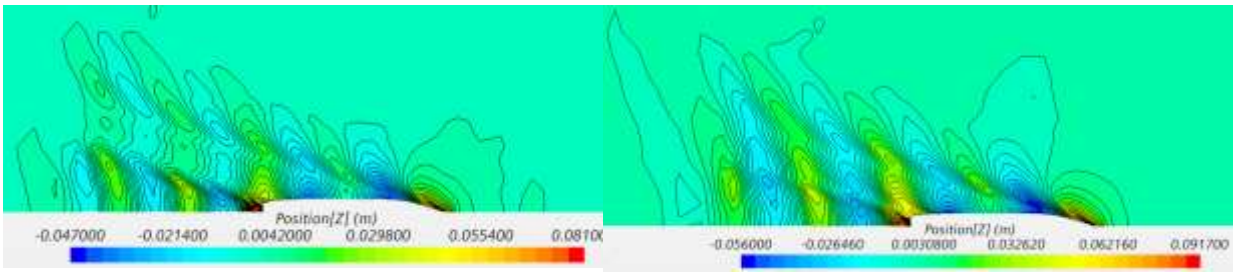

c) Fr=0.260 d) Fr=0.280

Figure 11. Predicted wave elevation patterns for the four Froude numbers

Figure 12 displays the wall shear stress distribution on the ship hull at four values of Froude number. It is clearly seen from Figure 12 that, the wall shear stress distribution on the ship hull occurs differently at different Froude numbers. However, the difference is not much. The wall shear stress increases as Froude number increases. The highest shear stress located at the fore part of the ship, especially at ship bow. The lowest wall shear stress located at ship stern.

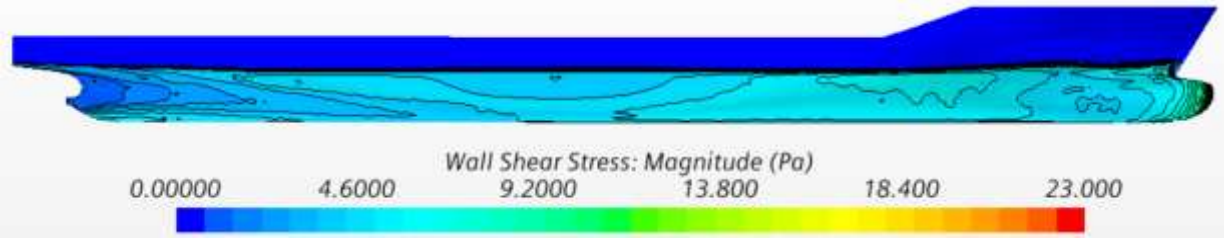

a) Fr=0.195

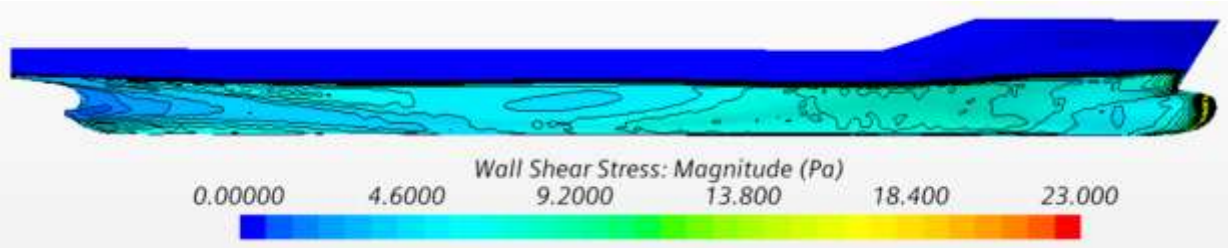

b) Fr=0.228

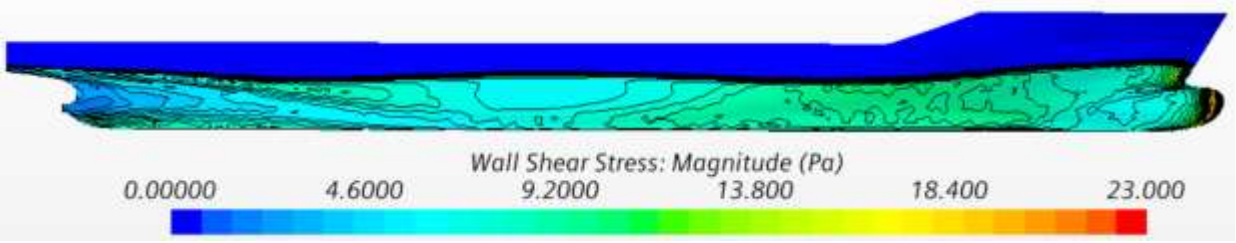

c) Fr=0.260

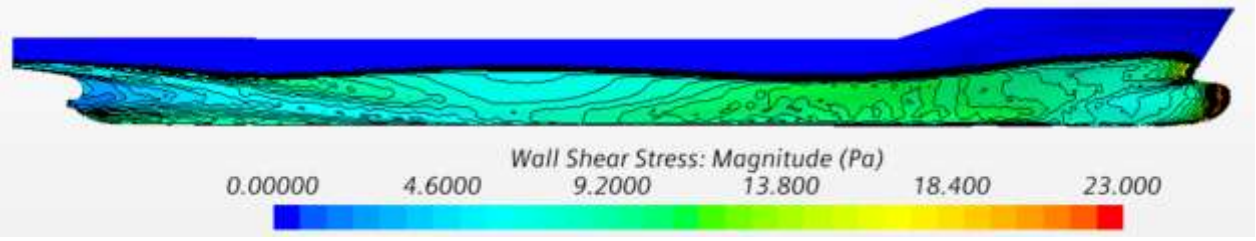

d) Fr=0.280

Figure 12. Predicted wall shear stress around the ship for the four Froude numbers

CONCLUSIONS

In this article, flow around a KCS containership in model scale is simulated using unsteady RANSE method. The presented simulation results indicated that using relatively medium mesh with about a million cells (for a half of the ship hull) and well created and locally refined mesh can achieve acceptable predicted values of total resistance, dynamic trim and sinkage. The Realizable k-ε turbulence model with wall functions is critically suitable for optimum results. The prism layers near the wall should be setup so that $y+$ values around 50 in order to obtain numerical results close to experimental results.

ACKNOWLEDGMENT

This research was funded by Thai Nguyen University of Technology, No. 666, 3/2 Street, Thai Nguyen, Viet Nam.

REFERENCES

[1] The 1978 ITTC Performance Prediction Method for Single Screw Ships https://ittc.info/media/2037/75-02-03-014.pdf.

[2] T.N. Tu, "Numerical prediction of propeller-hull interaction characteristics using RANS method", Polish Maritime Research, 2019.

[3] H.C. Raven, "Towards a CFD-based prediction of ship performance—progress in predicting full-scale resistance and scale effects", Vol. 150, Pp. A4, 2008.

[4] Y.K. Demirel, O. Turan, and A.J.A.O.R. Incecik, "Predicting the effect of biofouling on ship resistance using CFD". Vol. 62, Pp. 100-118, 2017.

[5] S. Bhushan, "Assessment of computational fluid dynamic for surface Combatant 5415 at Straight Ahead and Static Drift β= 20 deg", Vol. 141, No. 5, 2019.

[6] S. Bhushan, "Model-and full-scale URANS simulations of Athena resistance, powering, seakeeping, and 5415 maneuvering", Vol. 53, No. 4, Pp. 179-198, 2009.

[7] M.I. Roh, and K.Y. Lee, "Computational ship design", 2018: Springer.

[8] A.F. Molland, S.R. Turnock, and D.A. Hudson, "Ship resistance and propulsion", Cambridge university press, 2017.

[9] L. Larsson, and S.M. Engineers, "The Principles of Naval Architecture Series", ISBN: 978-0-939773-76-3, Ship resistance and flow. 2010.

[10] J.H. Ferziger, M. Perić, and R.L. Street, "Computational methods for fluid dynamics", Vol. 3. 2002: Springer.

[11] T.V. Nguyen, "Effects of Turbulence Models on the CFD results of Ship Resistance and Wake. in 日本船舶海洋工学会講演会論文集 Conference proceedings, the Japan Society of Naval Architects and Ocean Engineers. 2017.

[12] T. Yusuke, "Investigation on Effective Turbulence Models for Predicting Tanker Stern Flows", 6, Pp. 235-246, 2007.

[13] W.J. Kim, "Comparison of Turbulence Models for the Prediction of Wakes around VLCC Hull Forms", Vol. 5 (2), Pp. 27-48, 2001.

[14] H. Islam, and C.G. Soares, "Uncertainty analysis in ship resistance prediction using OpenFOAM", Ocean Engineering, Vol. 191, Pp. 105805, 2019.

[15] A. Shia, "Resistance calculation and motions simulation for free surface ship based on CFD", Procedia Engineering, Vol. 31, Pp. 68-74, 2012.

[16] C. Wu, L.Y. Z. Zhang, F. Zao, and K. Yan, "CFD simulation of ship model free to sigkage and trim advancing in Calm water. in Proceedings", Gothenburg 2000 workshop on numerical Ship hydrodynamic, 2010.

[17] T. Tu, "Numerical Prediction of Ship Resistance in Calm Water by Using RANS Method", Journal of Engineering and Applied Sciences, Vol. 13, No. 17, Pp. 7210-7214, 2018.

[18] B.J. Zhang, and S.L. Zhang, "Research on ship design and optimization based on simulation-based design (SBD) technique", 2019: Springer.

[19] J. Choi, "Resistance and propulsion characteristics of various commercial ships based on CFD results", Ocean engineering, Vol. 37, No. 7, Pp. 549-566, 2010.

[20] Z. Yong, "Turbulence model investigations on the boundary layer flow with adverse pressure gradients", Vol. 14, No. 2, Pp. 170-174, 2015.

[21] L. Larsson, F. Stern, and M. Visonneau, "Numerical ship hydrodynamics: an assessment of the Gothenburg 2010 workshop", 2013: Springer.

[22] Siemens, 2020. STAR-CCM+ User Guide.

[23] http://www.simman2008.dk/KCS/kcs_geometry.htm.

[24] ITTC, Recommended procedures and guidelines 7.5-03-02-04, 2014. Available from: https://ittc.info/media/4198/75-03-02-04.pdf.

[25] I.R. Procedures, Guidelines 7.5-03-02-03. Practical Guidelines for Ship CFD Applications, Revision, 2011. 1.

[26] S. Van, "Experimental investigation of the flow characteristics around practical hull forms. in Third Osaka Colloquium on Advanced CFD Applications to Ship Flow and Hull Form Design, Osaka, Japan, 1998.